International Journal of Thermal Sciences 59 (2012) 126–140

Contents lists available at SciVerse ScienceDirect

International Journal of Thermal Sciences

journal homepage: www.elsevier.com/locate/ijts

Effect of magnetic field on natural convection in a triangular enclosure filled with nanofluid

Amir Houshang Mahmoudi [a], Ioan Pop [b,*], Mina Shahi [c]

[a] Department of Mechanical Engineering, Faculty of Engineering, Semnan University, Semnan, Iran
[b] Department of Mathematics, Babeş-Bolyai University, 400048 Cluj-Napoca, CP 253, Romania
[c] Laboratory of Thermal Engineering, Faculty of Engineering Technology, University of Twente, Enschede, The Netherlands

A R T I C L E I N F O

Article history:
Received 15 October 2011
Received in revised form
16 March 2012
Accepted 9 April 2012
Available online 19 May 2012

Keywords:
Nanofluid
MHD
Natural convection
Numerical study
Triangular enclosure

A B S T R A C T

A numerical analysis of natural convection has been performed for a two-dimensional triangular enclosure with partially heated from below and cold inclined wall filled with nanofluid in presence of magnetic field. Governing equations are solved by finite volume method. Flow pattern, isotherms and average Nusselt number are presented for $0 < Ha < 100$, $10^4 < Ra < 10^7$, $0 < \phi < 0.05$ and six cases that are made by location of heat sources. The results show in presence of magnetic field flow field is suppressed and heat transfer decreases. Furthermore it is observed that maximum reduction of average Nusselt number in high value of Ha occurs at $Ra = 10^6$. It is found the nanoparticles are more effective at $Ra = 10^4$ where conduction is more pronounced.

1. Introduction

Magnetohydrodynamic (MHD) flow and especially when associated with heat transfer have received considerable attention recent years because of their wide variety of application in engineering areas such as crystal growth in liquid, cooling of nuclear reactor, electronic package, microelectronic devices, solar technology, etc. in case of free convection of an electrically conducting fluid in presence of magnetic field, there are two body force, buoyancy force and Lorentz force. They interact with each other an influence on heat and mass transfer, so it is important to study the detailed characteristics of transport phenomena in such a process to have a better product with improved design.

Several researches have been performed in recent years on the effect of the magnetic field on natural convection [1–4]. Kandaswamy et al. [1] studied magnetoconvection in a cavity with partially active vertical walls. They have considered nine different positions of active zone for different values of Ra and Ha number. They found the average Nusselt number decreases with an increase of Ha and increases with Grashof number. Also in large enough magnetic field the convection mode of heat transfer is converted into conduction mode. Pirmohammadi et al. [2] considered effect of magnetic field on convection heat transfer inside a tilted square enclosure. Their study showed heat transfer mechanism and flow characteristics inside the enclosure depend strongly upon both magnetic field and inclination angle. Grosan et al. [3] considered the inclination angel of magnetic field on the natural convection within a square cavity. It was found the convection mode depends upon both the strength and the inclination of the magnetic field. The applied magnetic field in the horizontal direction is most effective in suppressing the convection flow for a stronger magnetic field in comparison with the vertical direction. Natural convection in triangular enclosure has been subject of interest in many research studies due to its important application in various fields such as electronic components, solar collectors or roof/attics of buildings. Although there are some valuable studies in natural convection in triangular enclosure [5–8], but none of them considered the effect of magnetic field on the flow and heat transfer characteristics.

With the growing demand for efficient cooling systems, particularly in the electronics industry, more effective coolants are required to keep the temperature of electronic components below safe limits. Use of nanofluids is a potential solution to improve heat transfer [9]. Nanotechnology has been widely used in industry since materials with sizes of nanometers possess unique physical and chemical properties. Nano-scale particles added fluids are called as

* Corresponding author.
E-mail addresses: popm.ioan@yahoo.co.uk, pop.ioan@hotmail.com (I. Pop).

1290-0729/$ – see front matter © 2012 Elsevier Masson SAS. All rights reserved.
doi:10.1016/j.ijthermalsci.2012.04.006

Nomenclature

c_p	specific heat capacity (J/K)
g	gravitational acceleration(m/s^2)
Gr	Grashof number, $\beta g H^4 q''/(k\upsilon^2)_f$
H	height of the cavity (m)
Ha	Hartman number, $B_0 H \sqrt{(\sigma_f/\mu_f)}$
k	thermal conductivity (W/mK)
k_b	Boltzmann'sconstant, 1.38065×10^{-23}
Nu	Nusselt number
Nu^*	Nusselt ratio, $Nu_m/Nu_m|_{\phi=0}$
Nu^{**}	Nusselt ratio, $Nu_m/Nu_m|_{Ha=0}$
p	pressure (N/m^2)
P	dimensionless pressure,
Pr	Prandtl number, υ_f/α_f
Ra	Rayleigh number, $\beta g H^4 q''/(k\upsilon\alpha)_f$
T	temperature (K)
u,v	components of velocity (m/s)
U,V	Dimensionless of velocity component
W	width of the cavity (m)
x,y	Cartesian coordinates (m)
X,Y	dimensionless of Cartesian coordinates

Greek letters

α	thermal diffusivity, $k/(\rho c_p)$ (m^2/s)
β	coefficient of volume expansion (K^{-1})
ϕ	solid volume fraction
γ	electrical conductivity ratio, σ_s/σ_f
μ	dynamic viscosity (Pa.s)
θ	dimensionless temperature
ρ	density (kg/m^3)
σ	electrical conductivity
υ	kinematics viscosity (m^2/s)

Subscript

f	fluid
m	average
nf	nanofluid
o	reference state
s	solid
w	wall

nanofluid which is firstly introduced by Cho [9]. Use of metallic nanoparticles with high thermal conductivity will increase the effective thermal conductivity of these types of fluid remarkably. Since nanofluid consists of very small sized solid particles, therefore in low solid concentration it is reasonable to consider nanofluid as a single phase flow [10]. There are many numerical studies about heat and mass transfer of nanofluid in rectangular enclosure [11–18], in contrary, the number of studies on natural convection of nanofluid in triangular geometries is very limited [19–21].A numerical study of natural convection of copper–water nanofluid in a two-dimensional enclosure was done by Khanafer and Vafai [11]. The nanofluid in the enclosure was assumed to be in single phase. It was found in any given Grashof number, average Nusselt number in the enclosure increased with solid concentration. Mahmoudi et al. [12] investigated numerically the effect of position of horizontal heat source on the left vertical wall of a cavity filled with nanofluid. They found that presence of nanoparticles at low Ra is more pronounced and also when the heat source was located close to the top horizontal wall, the nanoparticles were more effective. Abu-Nada et al. [13] investigated the effect of nanofluid variable properties on the natural convection in enclosures. The variable thermal conductivity and variable viscosity models were compared to both the Maxwell-Garnett model and the Brinkman model. They found that at high Rayleigh numbers the average Nusselt number was more sensitive to the viscosity models than to the thermal conductivity models. Aminossadati and Ghasemi [20] have done numerical simulation of natural convective heat transfer in the triangular enclosure using nanofluid. They have considered the effect of position and dimension of heat source and apex angle on fluid flow and heat transfer. They found at low Rayleigh numbers, the heat transfer rate continuously increases with the enclosure apex angle and decreases with the distance of the heat source from the left vertex.

Magnetic nanofluid is a magnetic colloidal suspension of carrier liquid and magnetic nanoparticles. The advantage of magnetic nanofluid is that fluid flow and heat transfer can be controlled by external magnetic field, which makes it applicable in various fields such as electronic packing, thermal engineering and aerospace. In contrary to extensive studies on heat and mass transfer of nanofluid, only there are few studies that considered effect of magnetic field on nanofluid [22–24]. Hamad [22] has performed an analytical study on natural convection of a nanofluid over a linearly stretching sheet in presence of vertical magnetic field. He found for a given value of solid concentration, the heat transfer rate decreases as magnetic field increases. The point in this study is that the effective value of electric conductivity for nanofluid is not calculated and in the equations the electric conductivity is set according to properties of base fluid. So increase of solid volume fraction, in a selected magnetic field, doesn't effect on Lorenz force. Ghasemi et al. [24] numerically investigated the magnetic field effect on natural convection in a nanofluid-filled square enclosure. They have used basic mixture model for calculating effective electric conductivity of nanofluid. Their results showed the effect of the solid volume fraction on the heat transfer rate strongly depends on the values of the Rayleigh number and the Hartman number.

The present study has been motivated by the need to determine the detailed flow field, temperature distribution and natural convection heat transfer in a triangular enclosure filled with a nanofluid, in presence of magnetic field. A numerical analysis has been performed for a wide range of Rayleigh number, solid volume fraction and Hartman number. The effective thermal conductivity of nanofluid has been calculated using a model proposed by Patel [25]. The viscosity of nanofluid is calculated using the Brinkman [26] and also the effective electrical conductivity of nanofluid is modeled using Maxwell model [27]. In this paper results are presented in the form of streamlines, isotherms and average Nusselt number to show the effect of nanoparticles on the heat transfer and fluid flow in presence of magnetic field.

2. Problem definition and mathematical formulation

Fig. 1 displays schematically configuration of the two-dimensional triangular enclosure considered in this study. The diagonal wall is kept at a constant low temperature T_0 and the left vertical wall is assumed thermally adiabatic. Two heat sources with same length ($l = W/5$) are located on the bottom horizontal wall. For six cases, which are made with placement of heat source I and II, the heat transfer and fluid flow characteristics in different position of heat source are investigated. It is assumed that both the fluid phase and nanoparticles are in thermal equilibrium and there is no slip between them. Except for the density the properties of

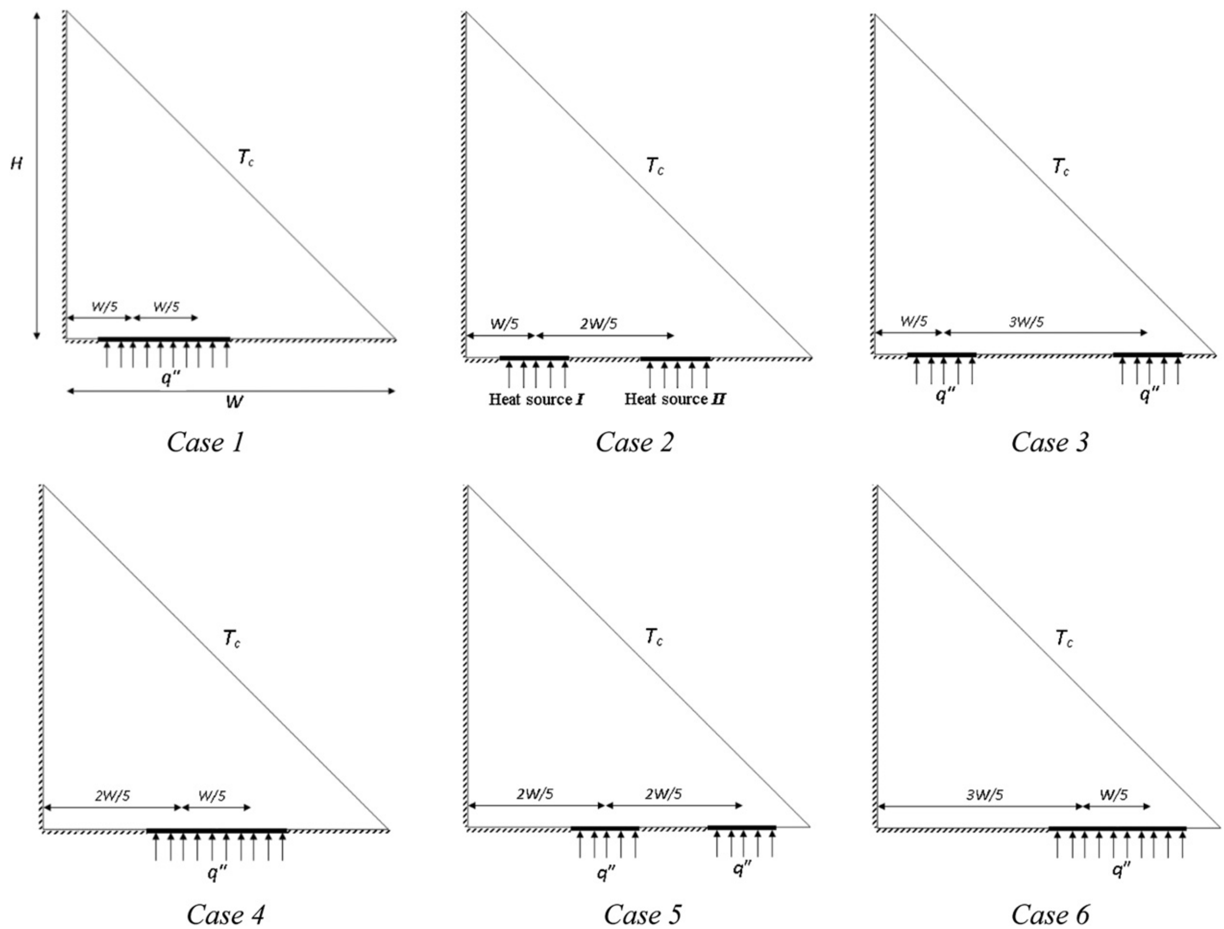

Fig. 1. Schematic configuration of the studied problems.

nanoparticles and fluid are taken to be constant. Table 1 presents thermophysical properties of water and copper at the reference temperature. It is further assumed that the Boussinesq approximation is valid for buoyancy force.

Under the above assumption, the conservation equation of mass, momentum and energy in a two-dimensional Cartesian coordinate system are

$$\frac{\partial u}{\partial x}+\frac{\partial v}{\partial y} = 0 \tag{1}$$

$$u\frac{\partial u}{\partial x}+v\frac{\partial u}{\partial y} = -\frac{1}{\rho_{\rm nf}}\frac{\partial p}{\partial x}+\upsilon_{\rm nf}\left(\frac{\partial^2 u}{\partial x^2}+\frac{\partial^2 u}{\partial y^2}\right) - \frac{\sigma_{\rm nf}B_0^2}{\rho_{\rm nf}}u \tag{2}$$

$$u\frac{\partial v}{\partial x}+v\frac{\partial v}{\partial y} = -\frac{1}{\rho_{\rm nf}}\frac{\partial p}{\partial y}+\upsilon_{\rm nf}\left(\frac{\partial^2 v}{\partial x^2}+\frac{\partial^2 v}{\partial y^2}\right) + \frac{g}{\rho_{\rm nf}}(T-T_\infty)\left[\phi\rho_{\rm s,0}\beta_{\rm s}+(1-\phi)\rho_{\rm f,0}\beta_{\rm f}\right] \tag{3}$$

$$u\frac{\partial T}{\partial x}+v\frac{\partial T}{\partial y} = \alpha_{\rm nf}\left(\frac{\partial^2 T}{\partial x^2}+\frac{\partial^2 T}{\partial y^2}\right) \tag{4}$$

Table 1
Thermophysical properties of water and copper.

Property	Water	Copper
c_p	4179	383
ρ	997.1	8954
k	0.6	400
β	2.1×10^{-4}	1.67×10^{-5}
σ	0.05	5.96×10^{7}

where $\alpha_{\rm nf} = k_{\rm nf}/(\rho c_{\rm p})_{\rm nf}$ is the effective thermal diffusivity of the nanofluid. Further, the effective density of nanofluid at the reference temperature can be defined as:

$$\rho_{\rm nf,0} = \left(1-\phi\right)\rho_{\rm f,o}+\phi\rho_{\rm s,o} \tag{5}$$

Which$\rho_{\rm nf,0}$,$\rho_{\rm f,0}$,$\rho_{\rm s,0}$ and ϕ are the density of nanofluid, density of base fluid, density of nanoparticles and volume fraction of the nanoparticles, respectively.

The heat capacity of nanofluid can be given as:

$$(\rho c_{\rm p})_{\rm nf} = \left(1-\phi\right)(\rho c_{\rm p})_{\rm f}+\phi(\rho c_{\rm p})_{\rm s} \tag{6}$$

The effective thermal conductivity of nanofluid is calculated using the Patel et al model [25]. as follows:

$$\frac{k_{\rm eff}}{k_{\rm f}} = 1+\frac{k_{\rm p}A_{\rm p}}{k_{\rm f}A_{\rm f}}+ck_{\rm p}Pe\frac{A_{\rm p}}{k_{\rm f}A_{\rm f}} \tag{7}$$

where c is constant and must be determined experimentally (for the current study $c = 3.6 \times 10^4$ [25]), $A_{\rm p}/A_{\rm f}$ and Pe here is defined as:

$$\frac{A_{\rm p}}{A_{\rm f}} = \frac{d_{\rm f}}{d_{\rm p}}\frac{\phi}{(1-\phi)} \quad , \quad Pe = \frac{u_{\rm p}d_{\rm p}}{\alpha_{\rm f}} \tag{8}$$

where $d_{\rm p}$ is diameter of solid particles that in this study is assumed to be equal to 100 nm, $d_{\rm f}$ is the molecular size of liquid that is taken as 2Å for water. Also $u_{\rm p}$ is the Brownian motion velocity of nanoparticle which is defined as:

$$u_{\rm p} = \frac{2{\rm k_b}T}{\pi\mu_{\rm f}d_{\rm p}^2} \tag{9}$$

where $k_{\rm b}$ is the Boltzmann constant.

The effective viscosity of nanofluid is calculated using the Brinkman model [26],

$$\mu_{\mathrm{nf}} = \frac{\mu_{\mathrm{f}}}{(1-\phi)^{2.5}} \tag{10}$$

The effective electrical conductivity of nanofluid was presented by Maxwell [27] as below

$$\frac{\sigma_{\mathrm{nf}}}{\sigma_{\mathrm{f}}} = 1 + \frac{3(\gamma-1)\phi}{(\gamma+2)-(\gamma-1)\phi} \tag{11}$$

where $\gamma = \sigma_{\mathrm{s}}/\sigma_{\mathrm{f}}$

In order to estimate the heat transfer enhancement, we have calculated the local Nusselt number (Nu) and the average Nusselt number (Nu_{m}) for the heat source wall as follows:

$$Nu = \frac{1}{\theta|_{\text{heat source wall}}} \tag{12}$$

$$Nu_m = \frac{\int_{\text{Fins surfaces}} Nu\, dn}{\int_{\text{Fins surfaces}} dn} \tag{13}$$

Eqs. (1)–(4) can be converted to the dimensionless form by definition of the following parameters as:

$$X = \frac{x}{H}, \quad Y = \frac{y}{H}, \quad U = \frac{uH}{\alpha_{\mathrm{f}}}, \quad V = \frac{vH}{\alpha_{\mathrm{f}}}, \quad \theta = \frac{(T-T_{\mathrm{C}})k_{\mathrm{f}}}{q''H},$$
$$P = \frac{p}{\rho_{\mathrm{nf}}}\frac{H^2}{\alpha_{\mathrm{f}}^2} \tag{14}$$

Therefore using the above parameters leads to dimensionless form of the governing equations as below:

$$\frac{\partial U}{\partial X} + \frac{\partial V}{\partial Y} = 0 \tag{15}$$

$$U\frac{\partial U}{\partial X} + V\frac{\partial U}{\partial Y} = -\frac{\partial P}{\partial X} + \frac{\mu_{\mathrm{nf}}}{\rho_{\mathrm{nf}}\alpha_{\mathrm{f}}}\left(\frac{\partial^2 U}{\partial X^2} + \frac{\partial^2 U}{\partial Y^2}\right) - Ha^2.Pr.\frac{\sigma_{\mathrm{nf}}}{\sigma_{\mathrm{f}}}.\frac{\rho_{\mathrm{f}}}{\rho_{\mathrm{nf}}}U \tag{16}$$

$$U\frac{\partial V}{\partial X} + V\frac{\partial V}{\partial Y} = -\frac{\partial P}{\partial Y} + \frac{\mu_{\mathrm{nf}}}{\rho_{\mathrm{nf}}\alpha_{\mathrm{f}}}\left(\frac{\partial^2 V}{\partial X^2} + \frac{\partial^2 V}{\partial Y^2}\right)$$
$$+ Ra.Pr.\frac{\rho_{\mathrm{f},0}}{\rho_{\mathrm{nf},0}}\left(1 - \phi + \phi\frac{\rho_{\mathrm{s}}\beta_{\mathrm{s}}}{\rho_{\mathrm{f}}\beta_{\mathrm{f}}}\right)\theta \tag{17}$$

$$U\frac{\partial \theta}{\partial X} + V\frac{\partial \theta}{\partial Y} = \frac{\alpha_{\mathrm{nf}}}{\alpha_{\mathrm{f}}}\left(\frac{\partial^2 \theta}{\partial X^2} + \frac{\partial^2 \theta}{\partial Y^2}\right) \tag{18}$$

3. Numerical method and validation

The dimensionless equations have been solved numerically based on the finite volume method using a collocated grid system. Central difference scheme is used to discretize the diffusion terms whereas upwind difference is adopted for the convection terms. The resulting discretized equations have been solved iteratively through strongly implicit procedure (SIP) [28]. The SIMPLE algorithm [29] has been adopted for the pressure velocity coupling. To check the convergence of the sequential iterative solution, the sum of the absolute differences of the solution variables between two successive iterations has been calculated. Solution is assumed converged when this summation falls below the convergence criterion which is chosen as 10^{-6} in this study. In this study, a regular rectangular domain is used. The inclined wall of the enclosure is approximated with stair case-like zigzag lines and the grid cells outside of the triangular domain are assumed inactive. This method has been used before by Asan and Namli [5], Varol et al. [7], ghasemi and Aminossadati [19,20]. To allow grid-independent examination, the numerical procedure has been conducted for different grid resolutions. Table 2 demonstrates the influence of number of grid points for a test case of fluid confined within the present configuration. The results show that the grid system of 121 × 121 is fine enough to obtain accurate results.

The results have been validated for the natural convection flow in an enclosed cavity filled by a pure fluid, as reported by de Vahl Davis [30] to observe a good agreement; see Table 3. Another test for validation of the current code was performed for the case of natural convection in a rectangular enclosure in the presence of magnetic field. In this test case, the average Nusselt number using different Gr and Ha number have been compared with those obtained by Venkatachalappa et al. [31] as shown in Table 4 and a good agreement with the results was registered. The present computation also is validated against the results of Akinsete and Coleman [32], Asan and Namli [5], Varol et al. [7], Ghasemi and Aminossadati [19] for natural convection within the triangular enclosure with $AR = 0.25$ and $Ra = 2772$ (Fig. 2).

4. Results and discussion

A numerical study has been performed through finite volume method to analyze the laminar natural convection heat transfer and fluid flow in triangular enclosure in presence of vertical magnetic field using CuO-water nanofluid. Streamlines, Isotherms and average Nusselt number are presented for a wide range of Ra, Ha and ϕ ($10^4 < Ra < 10^7$, $0 < Ha < 100$, $0 < \phi < 0.05$) for six cases.

The results depicted in Figs. 3 to 8 demonstrate the influence of magnetic field on the fluid flow and the temperature distribution in the enclosure for each case at different Ra and $\phi = 0$. At $Ra = 10^5$ and $Ha = 0$ as can be seen in Fig. 3, the fluid rises up along the side of left vertical wall and flows down along the cooled diagonal wall and forms a clock-wise rotating cell within the cavity in each case except case 6 that is made two small vortexes at corner of cavity. It is observed as the heat sources become closer to the diagonal wall the flow intensity decreases. At case 1 although the heat sources place at farthest location respect to diagonal wall and velocity of recirculation flow is higher than other cases but the long distance between heat sources and cold wall leads to lower amount of heat transfer. Therefore, moving heat sources toward the diagonal wall results in a decrease in the strength of the circulating cells, but due to shorter distance with low temperature source and stronger conduction, heat transfer increases and hence the temperature of heat sources surfaces decreases. Although at case 6 conduction is strong but since heat source surface is covered by two pretty weak cells, the convection is weak, So in comparison with case 3 and 5

Table 2
Result of grid independence examination.

Number of grids in X–Y	Nu
41 × 41	9.216
61 × 61	9.163
81 × 81	9.072
101 × 101	9.010
121 × 121	8.971
141 × 141	8.944

Table 3
Comparison of results obtained in this study by [30].

Nu_m			
	Present	de Vahl Davis [30]	Error (%)
$Ra = 10^4$	2.248	2.242	0.267
$Ra = 10^5$	4.503	4.523	0.444
$Ra = 10^6$	9.147	9.035	1.24

that only the heat sources *II* is close to the diagonal wall, heat transfer is lower and surface temperature is higher. When the magnetic field is imposed on the enclosure, the velocity field suppressed owing to the retarding effect of the Lorenz force. So intensity of convection weakens significantly. The braking effect of the magnetic field is observed from the maximum stream function value. At case 4 and 5, with increase of *Ha* a clock-wise circulating cell starts to develop in the left side of heat source I that is in contact with the main circulating cell. It is worth noting that in high Hartman number, velocity field suppresses significantly and conduction is dominant, so at case 6 that convection is weak even in absence of magnetic field conduction is stronger compared to other cases, lowest reduction in heat transfer happen.

As *Ra* increases, the buoyant force becomes stronger and velocity increases, also the isotherms are deformed due to convection mode being to play a more significant role with increasing the flow velocity. At case 3 and 5 that heat source *II* is close to diagonal wall, with increase of *Ra* from 10^5 to 10^6 a pair of weak counter rotating cell appears on the surface of heat source *II* and causes a reduction in enhancement of heat transfer with increase of *Ra* compared to other cases. For example with increase of *Ra* to 10^6, surface temperature of heat source *II* at case 4 decreases from approximately 0.18 to 0.1 but at case 5 it decreases from 0.1 to 0.08. Fig. 5 shows that at case 1 with increase of *Ha* value, the enclosure is mainly associated with one clock-wise circulation zone, but at other cases as Hartman number increases, either the unicellular pattern turns out to be multicellular (case 4 and 5) or the initial single cell formation splits into dual cells (case 2). At case 6 the two triangular cells at the corners of cavity grow in size with *Ha* and squeeze the main cell so its contact with diagonal wall decreases. As can be seen in Fig. 6, at $Ra = 10^6$ convection is still dominant in low value of *Ha*, but as Hartman number increases further the isothermal lines inside the cavity approach more and more toward the conduction like distribution pattern and become parallel to the diagonal wall.

The results for higher Rayleigh number are presented in Figs. 7 and 8. At $Ra = 10^7$ and $Ha = 0$ except case 6, the circulating cells that sweep heat sources surface, directly contact the diagonal wall. So the heat transfers directly from heat source to low temperature source. But at case 6, the CCW rectangular cell that covers most part of heat sources surface, only in a small boundary is in contact with diagonal wall and leads to a reduction in heat transfer. So in this case the surface temperature of heat sources in spite of being closer to the diagonal wall, but is higher compared to other cases. So that surface temperature of heater at case 6 is about 0.08 but at case 1, that was the worst case from heat transfer point of view in lower Rayleigh number, is about 0.06. With increase of *Ha*, the CCW cell is stretched in the upward vertical direction and squeezes the upper cell and finally at $Ha = 100$ removes it. At case 2 and absence of magnetic field or even at $Ha = 10$, a small CCW cell is placed at the top of the cavity. As magnetic field is increased further, this cell disappears and a pair of counter rotating eddies of almost same size appears at the right side of the main circulating cell. Applying magnetic field at $Ra = 10^7$ for case 1 and 4 causes the same manner as explained for $Ra = 10^6$. At case 5 as Hartman number increases the small cells enlarged and to be stretched in upward vertical direction, so two pair of counter rotating cells cover whole enclosure area. Unlike Figs. 4 and 6 which the isotherms become uniform at strong magnetic field indicating conduction regime, it is observed in Fig. 8 that even for high Hartman number at $Ra = 10^7$, the convection regime is still dominant.

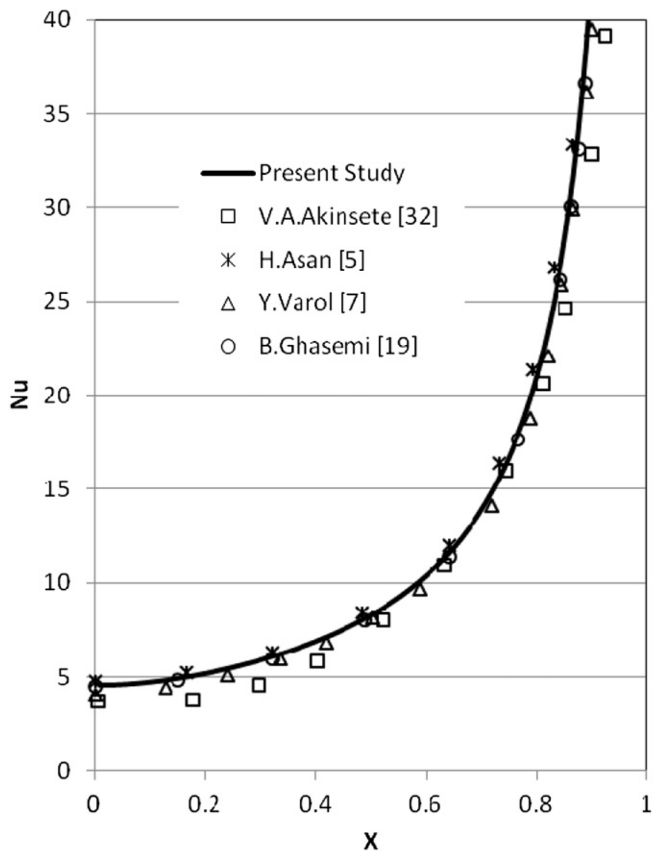

Fig. 2. Comparison of results of local Nusselt numbers for triangular enclosure.

Table 4
Comparison of average Nusselt number with previous works for different *Gr* number.

	Ha	Present study	Venkatachalappa et al. [31]	Error %
$Gr = 10^4$	0	2.5294	2.5188	0.42
	10	2.2375	2.2234	0.63
	50	1.0884	1.0856	0.26
	100	1.0132	1.0132	0.22
$Gr = 10^5$	0	5.0787	4.9198	3.23
	10	4.9681	4.8053	3.39
	50	2.9894	2.8442	5.1
	100	1.4785	1.4317	3.27

In order to obtain a better understanding of the flow behavior within the enclosure in presence of magnetic field, the vertical velocity component at $Y = 0.3$ and $\phi = 0$ are plotted in Fig. 9 for case 3. At $Ra = 10^5$ after the magnetic field is applied, the maximum vertical velocity decreased strongly due to Lorenz force effect. So that at $Ha = 100$, the vertical velocity profile is almost flat. At $Ra = 10^7$ since flow is strong, the low value of *Ha* does not have a considerable effect on vertical velocity profile. At $Ha = 100$ although velocity decreases but in comparison with $Ra = 10^5$, it is observed even for high Hartman number, vertical velocity component has a considerable value, indicating lower effect of magnetic field on flow field at higher Rayleigh number.

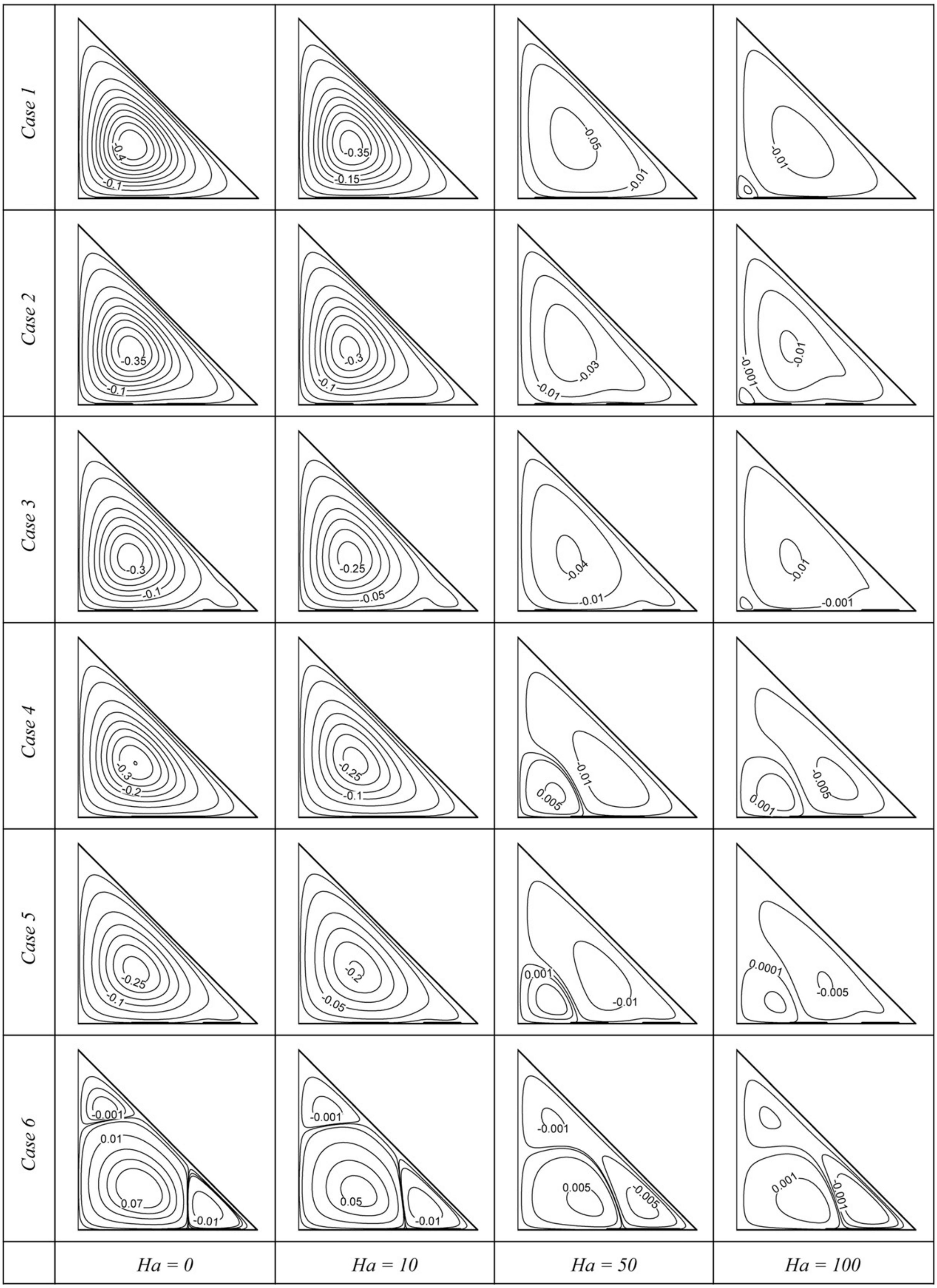

Fig. 3. Streamlines at $Ra = 10^5$ for different Hartman numbers and $\phi = 0$.

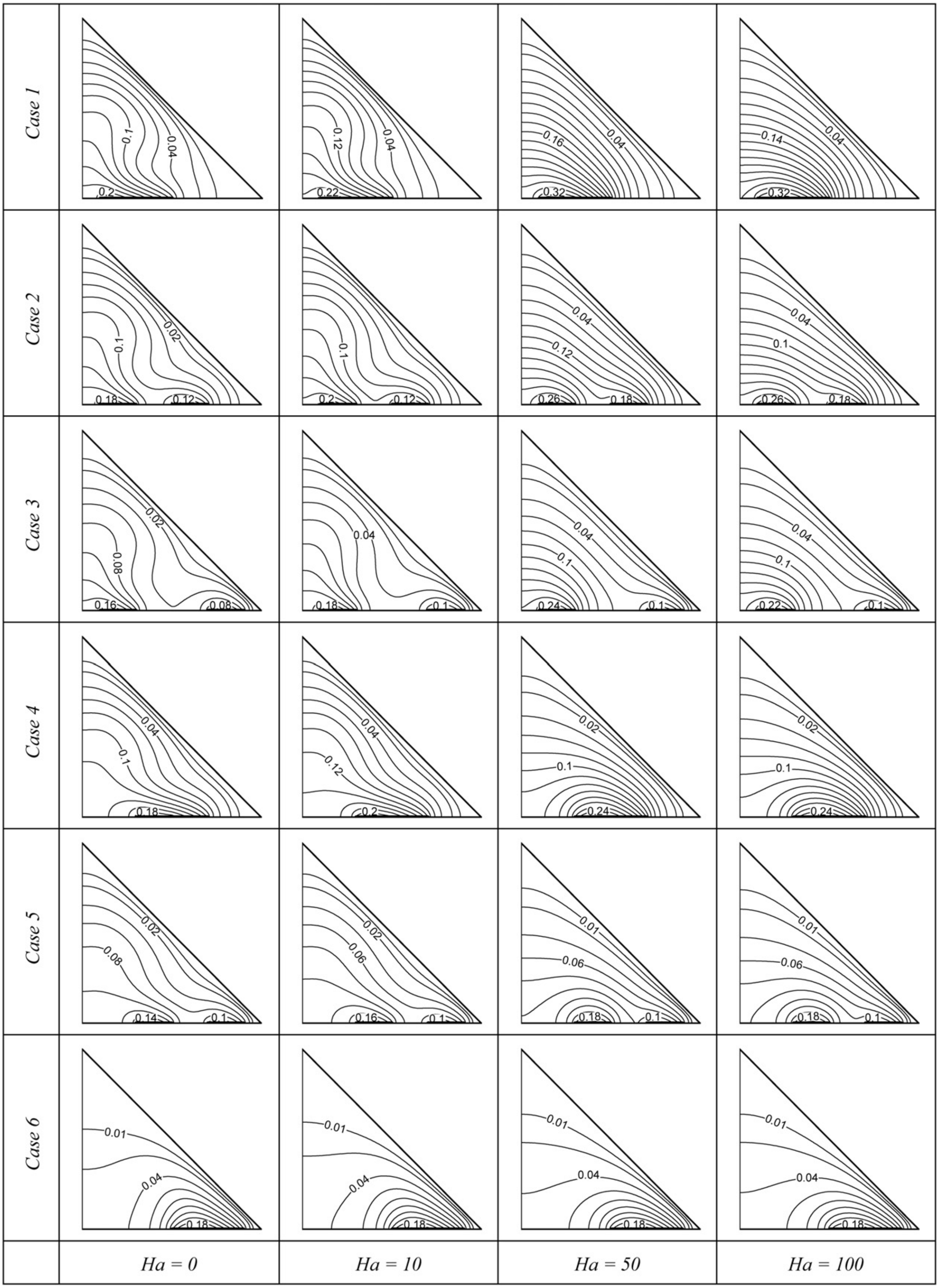

Fig. 4. Isothermal lines at $Ra = 10^5$ for different Hartman numbers and $\phi = 0$.

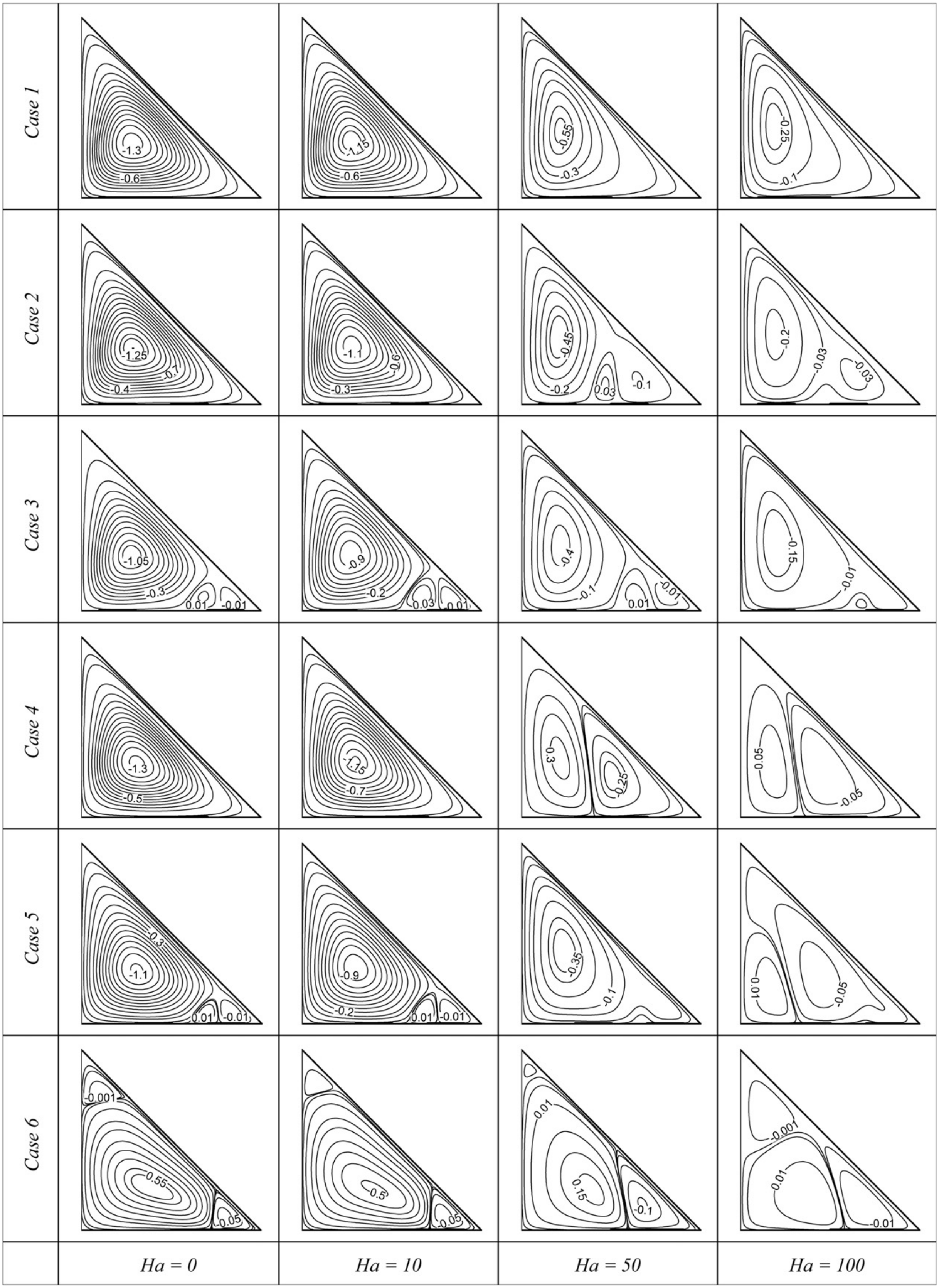

Fig. 5. Streamlines at $Ra = 10^6$ for different Hartman numbers and $\phi = 0$.

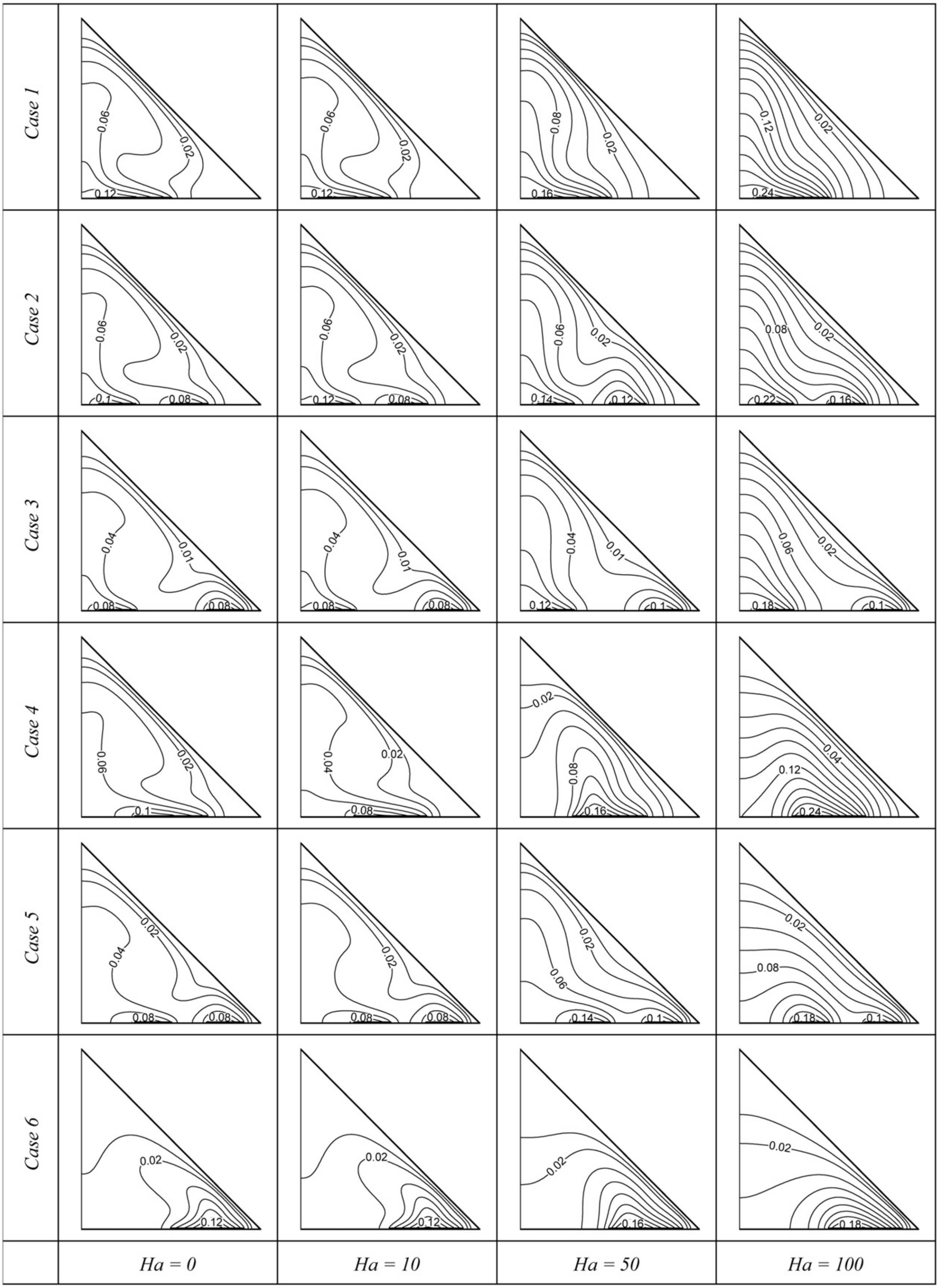

Fig. 6. Isotherms at $Ra = 10^6$ for different Hartman numbers and $\phi = 0$.

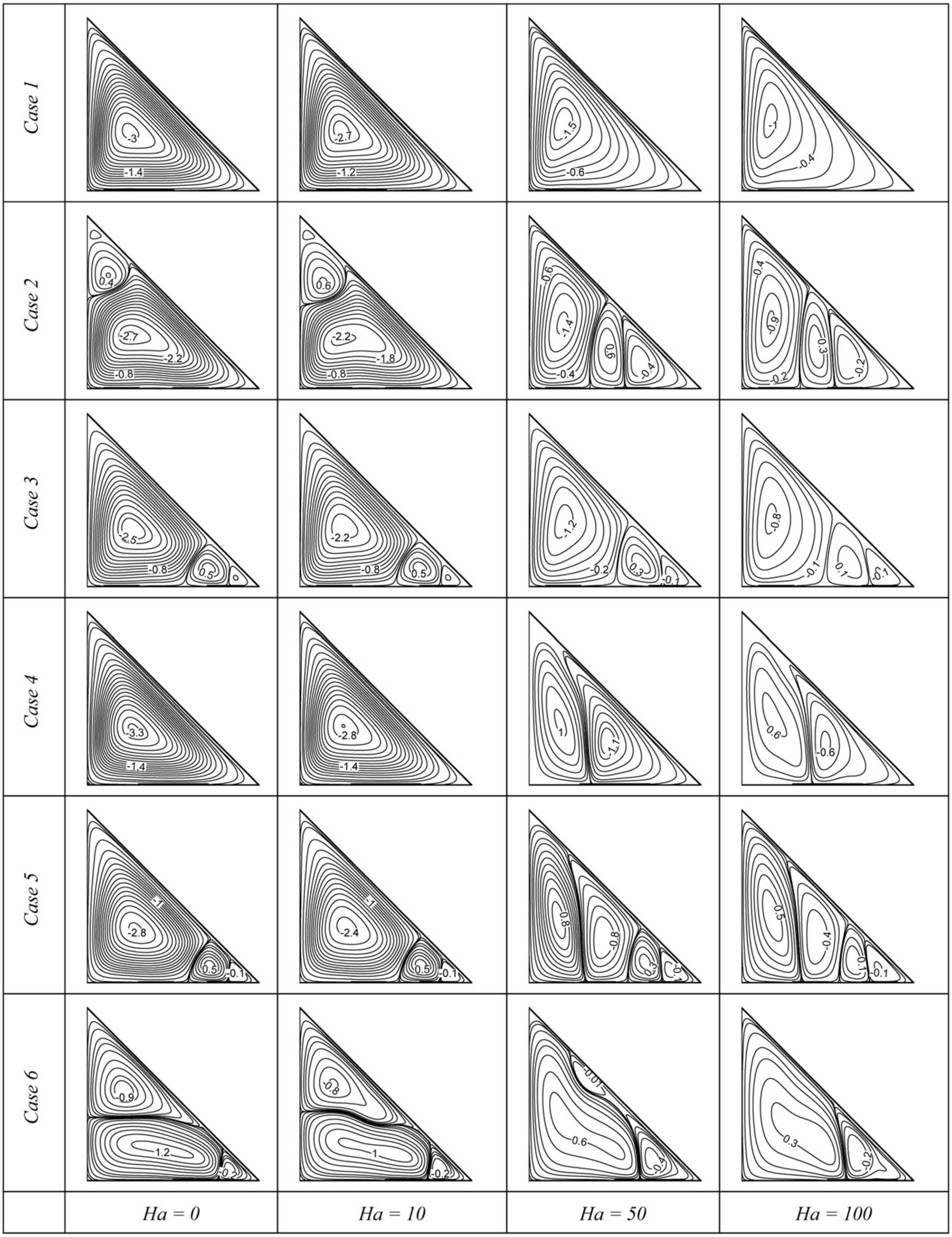

Fig. 7. Streamlines at $Ra = 10^7$ for different Hartman numbers and $\phi = 0$.

Fig. 10 illustrates the impact of nanoparticles on the vertical velocity at $Y = 0.3$ for case 3. Presence of metallic nanoparticles has three effects on heat transfer and fluid flow. Nanoparticles enhance thermal conductivity of base fluid so heat transfer and hence buoyancy force increases which leads to an augmentation in heat transfer. The second effect of nanoparticles is increase of viscosity that leads to a reduction in kinetic energy and attenuation of the flow field. As a third effect, nanoparticles increase the effective

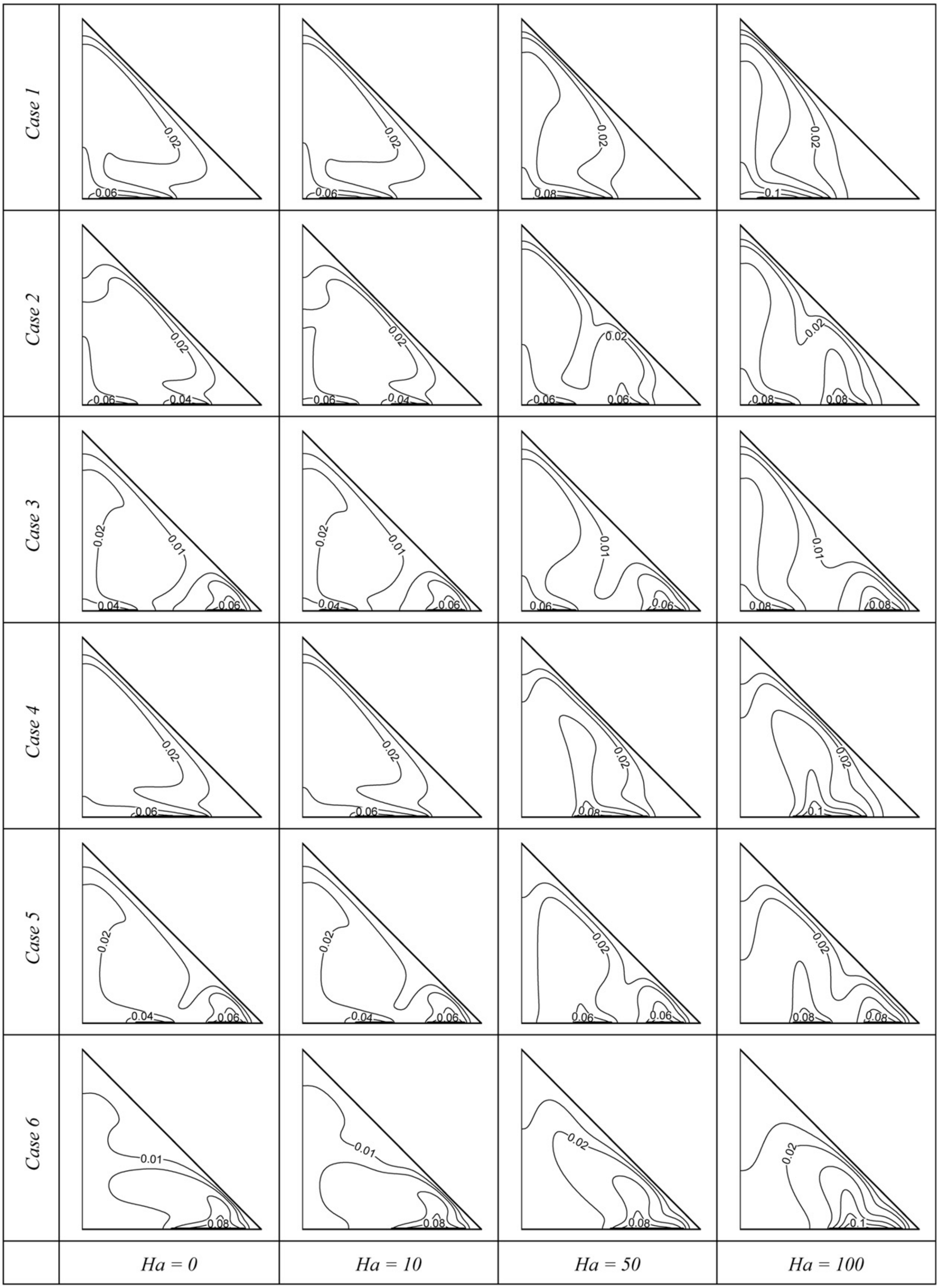

Fig. 8. Isothermal lines at $Ra = 10^7$ for different Hartman numbers and $\phi = 0$.

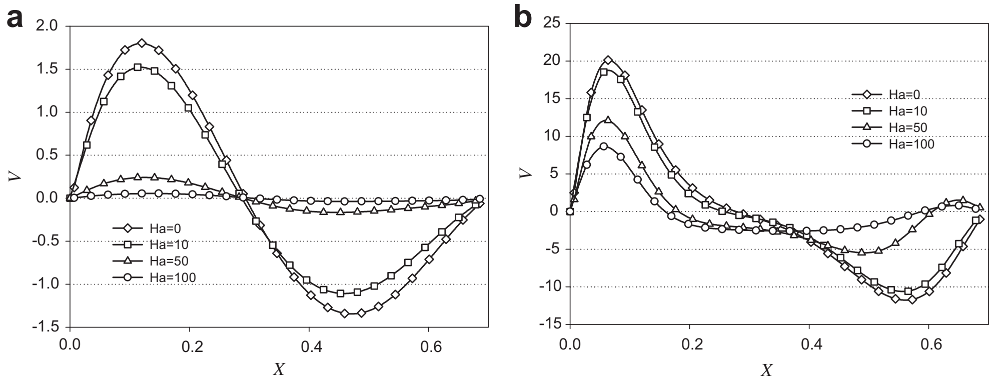

Fig. 9. Variation of vertical velocity at $Y = 0.3$ with Hartman number for case 3 a) $Ra = 10^5$ b) $Ra = 10^7$.

eclectic conductivity and lead to enhance the Lorenz force so it causes a reduction in flow intensity and heat transfer. Results in the Fig. 10 indicate that increase of nanoparticles intensifies the flow field. At $Ra = 10^5$ and in presence of relatively strong magnetic field ($Ha = 50$) the velocity field is too week, so enhancement of velocity due to presence of nanoparticles is negligible. The effect of nanoparticles on flow intensity is more pronounced at higher Rayleigh number that increase of viscosity effect in comparison with strong flow field is negligible. So, that at $Ha = 0$ and $Ra = 10^7$ with 5% solid concentration the maximum vertical velocity increases about 40% but at $Ra = 10^5$ it increases only 17%.

The results depicted in Fig. 11 demonstrate local Nusselt number along the heat sources for pure fluid at $Ra = 10^5$ and $Ha = 0$. For all cases, a sharp variation in local Nusselt number is observed near the edges of heat source. This is due to the heat transfer rate increases from zero on the thermally insulated south wall to the maximum value at the edge of the heat sources. It is observed, due to shorter distance between right edge of heat source with diagonal wall and also since the cold flow at first contact with this edge, so heat transfer and the local Nusselt number in this area is higher than left edge. It is interesting to note that at case 6 the value of local Nusselt number at the middle of heater I ($X = 0.6$) decreases more than other cases. This due to the fact that two week counter cells form on the heat source and make stagnation point vicinity of $X = 0.6$ and leads to considerable reduction in the heat transfer and Nusselt number as well. At case 3 due to heat source *II* respect to case 2 is closer to cold wall, heat transfer form heater *II* is higher and hence the temperature of the heater surface and the fluid that is in contact with heater in lower. Then the fluid with lower temperature pass over the heater I and absorb more energy compared to case 2,in spite of the heater I is placed in a same position in both cases. So as can be seen clearly in Fig. 11-b the local Nusselt number of heater I for case 3 in higher than case 2.

The analysis of heat transfer from the enclosure is carried out by examine the variation of the average Nusselt number along the heat source. Average Nusselt number is plotted as a function of solid

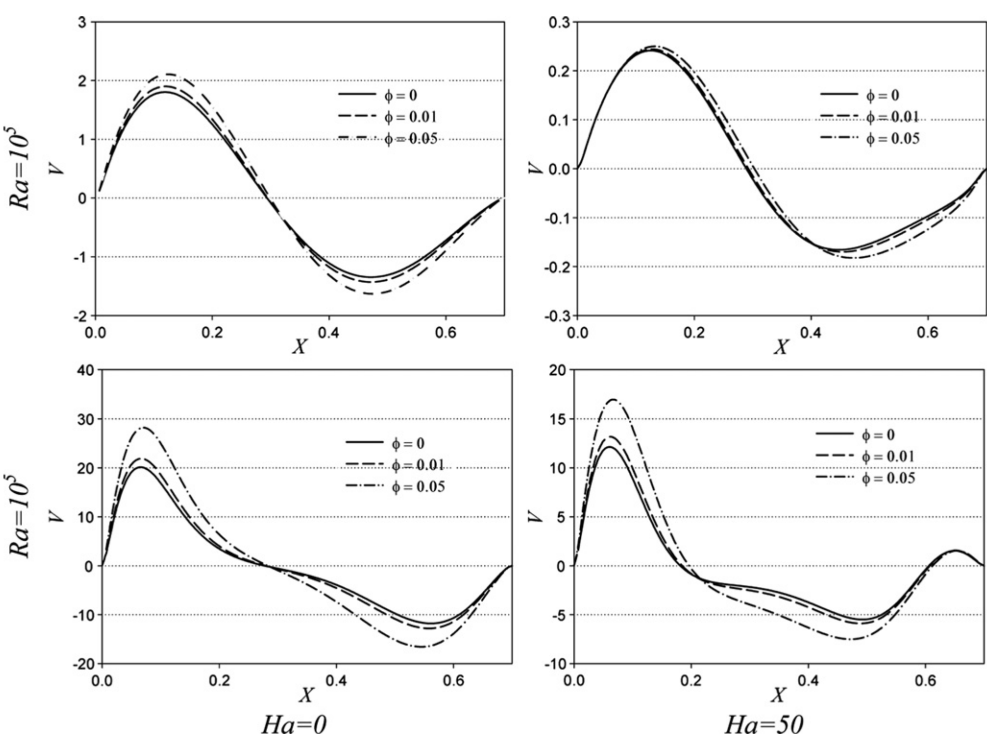

Fig. 10. Variation of y-velocity at $Y = 0.3$ with solid concentration for case 3 at different *Ra* and *Ha*.

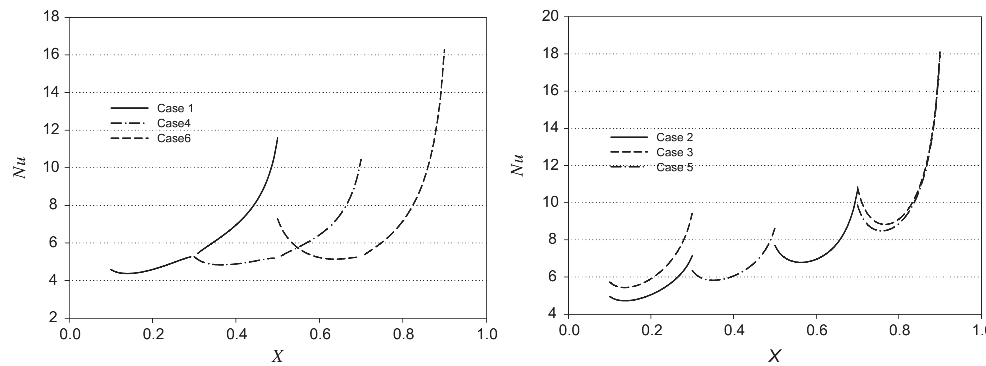

Fig. 11. Local Nusselt number along the heat sources at $Ra = 10^5$ and $Ha = 0$ for pure fluid.

concentration in Fig. 12 at different values of Hartman and Rayleigh number for case 3. As it is expected, the average Nusselt number increases with *Ra*. Increase of solid concentration leads to enhancement of thermal conductivity and so increases heat transfer from heat source and the Nu_m as well. As shown in the Fig. 12, the presence of nanoparticles in low Rayleigh number, where the heat transfer is dominated by conduction, causes better enhancement in heat transfer. So that at $Ra = 10^4$ and $Ha = 0$ using 5% solid concentration, the average Nusselt number increases by 50% compared to 30% for the case of $Ra = 10^7$. As it is presented in Figs. 3 and 9, at$Ra = 10^5$ with increase of *Ha* the convection significantly suppressed so that at $Ha = 50$ conduction in dominant completely. This leads to Nu_m at $Ra = 10^5$ for high value of *Ha*, is equal to the value of Nu_m at $Ra = 10^4$ and has the same manner with presence of nanoparticles.

Variation of average Nusselt number as a function of Rayleigh for different value of *Ha*, is presented in Fig. 13 for pure fluid. It can be seen clearly at each cases and *Ra*, the average Nusselt number decreases as Hartman number increases. This is expected due to presence of magnetic field retarded the velocity field and hence convection and Nusselt number decreases. At $Ra = 10^4$ since the flow field is week, the presence of magnetic field has a negligible effect on flow and so average Nusselt number is almost constant. At high *Ra*, due to strong flow field, the braking effect of low magnetic field is less than moderate *Ra*. So in all cases except case 6, the maximum reduction in average Nusselt number for $Ha = 10$ happen at $Ra = 10^5$. At case 6, as it was presented in Figs. 3 and 4, even in absence of magnetic field flow intensity is lower than other cases. With increase of *Ha*, although the convection is suppressed, but because even at $Ha = 0$ most part of heat transfer is done by conduction due to short distance with cold wall, the Nu_m decreases less than other cases. So, that at $Ha = 100$ Nusselt is reduced only 3% compared to $Ha = 0$. At $Ra = 10^5$ and $Ha = 50$ heat is transferred almost by pure conduction, so more enhancement of magnetic field

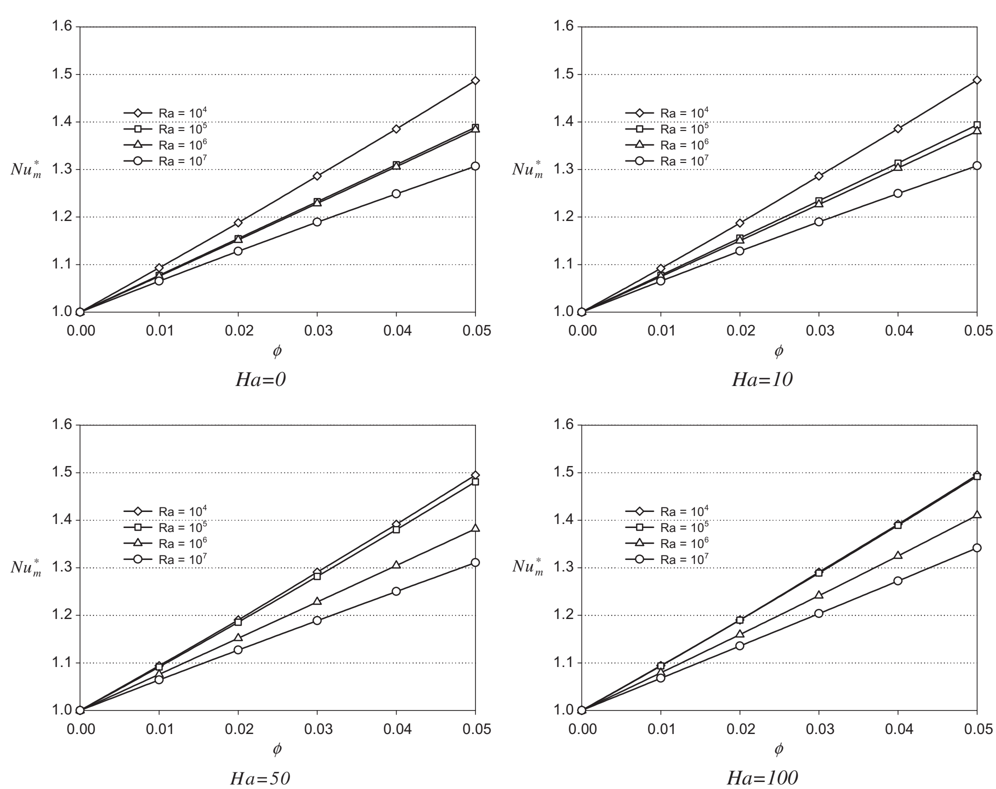

Fig. 12. The effect of solid concentration on the variation of the average Nusselt number for different values of Rayleigh and Hartman numbers in case 3.

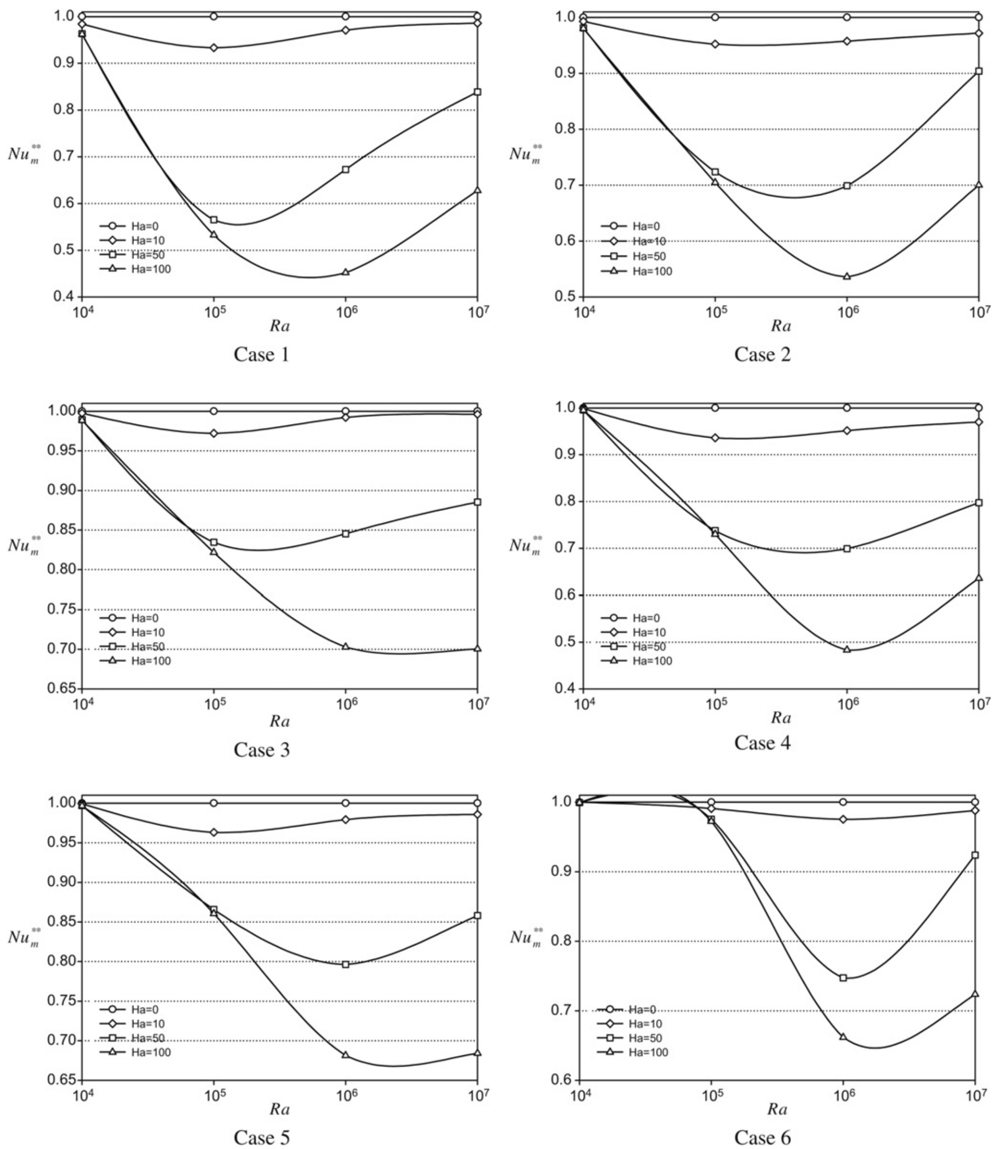

Fig. 13. The effect of Hartman number on the variation of the average Nusselt number for different values of Rayleigh.

doesn't affect heat transfer and hence Nu_{m} is kept constant. But at $Ra = 10^6$ flow field is stronger and further increase of Ha results in more reduction in convection and Nu_{m}. on the contrary, at $Ra = 10^7$ due to the flow intensity is very high, even at $Ha = 100$ the velocity has a considerable value and so magnetic field has less effect on heat transfer. Therefore as it is clearly observed in Fig. 13, at high Hartman number the maximum reduction in Nu_{m} takes place at $Ra = 10^6$. The results indicate the lowest and highest effect of magnetic field on the Nusselt at $Ra = 10^6$ are in case 3 and case 1 respectively with 30% and 55% as a result of enhancement of Ha to 100.

5. Conclusion

The model was applied to simulate the natural convection in a triangular subjected to the copper–water nanofluid in presence of vertical magnetic field. The geometry considered is a two-dimensional cavity with two identical heat sources on the horizontal wall and the diagonal wall is kept at constant low temperature. The results were presented for $10^4 < Ra < 10^7$, $0 < Ha < 100$ and$0 < \phi < 0.05$ in form of streamlines, isotherms and average Nusselt number. In view of the obtained results, following findings may be summarized.

The lowest heat transfer is observed at case 1 and the highest amount of heat transfer is done at case 3 and 5. At $Ra = 10^5$ and $Ha = 0$ the average Nusselt number at case 5 is approximately 38% more than case 1, but in higher value of Ra, this difference decreases, so that at $Ra = 10^7$ it reaches to 12%. Presence of nanoparticles is more effective at low Rayleigh number where conduction is more pronounced. With increase of Ha the velocity field in whole cases is suppressed and leads to reduction in heat transfer and average Nusselt number. At $Ra = 10^4$ the Nusselt number becomes constant with Ha, since even in absence of magnetic field flow filed is very week and conduction is dominant. In high value of Ha, the most reduction in Nu_{m} occurs at $Ra = 10^6$, the highest and lowest effect was observed in case 3 and case 1 respectively. At $Ra = 10^5$ and strong magnetic field, the convection is suppressed completely and conduction is dominant, so the value of Nu_{m} is equal to $Ra = 10^4$ and the effect of nanoparticles on enhancement of Nu_{m} is the same.

References

[1] P. Kandaswamy, S.M. Sundari, N. Nithyadevi, Magnetoconvection in an enclosure with partially active vertical walls, International Journal of Heat and Mass Transfer 51 (2008) 1946–1954.

[2] M. Pirmohammadi, M. Ghassemi, Effect of magnetic field on convection heat transfer inside a tilted square enclosure, International Communications in Heat and Mass Transfer 36 (2009) 776–780.

[3] T. Grosan, C. Revnic, I. Pop, D.B. Ingham, Magnetic field and internal heat generation effects on the free convection in a rectangular cavity filled with a porous medium, International Journal of Heat and Mass Transfer 52 (2009) 1525–1533.

[4] N. Nithyadevi, P. Kandaswamy, S.M. Sundari, Magnetoconvection in a square cavity with partially active vertical walls: time periodic boundary condition, International Journal of Heat and Mass Transfer 52 (2009) 1945–1953.

[5] H. Asan, L. Namli, Laminar natural convection in a pitched roof of triangular cross-section: summer day boundary conditions, Energy and Buildings 33 (2000) 69–73.

[6] A. Omri, M. Najjari, S.B. Nasrallah, Numerical analysis of natural buoyancy-induced regimes in isosceles triangular cavities, Numerical Heat Transfer, Part A 52 (2007) 661–678.

[7] Y. Varol, H.F. Oztop, A. Koca, Entropy production due to free convection in partially heated isosceles triangular enclosures, Applied Thermal Engineering 28 (2008) 1502–1513.

[8] Y. Varol, H.F. Oztop, I. Pop, Entropy generation due to natural convection in non-uniformly heated porous isosceles triangular enclosures at different positions, International Journal of Heat and Mass Transfer 52 (2009) 1193–1205.

[9] S.U.S. Cho, Enhancing thermal conductivity of fluids with nanoparticles, ASME Fluids Engineering Division 231 (1995) 99–105.

[10] Y.M. Xuan, Q. Li, Heat transfer enhancement of nanofluid, International Journal of Heat and Fluid Flow 21 (2000) 58–64.

[11] Khalil Khanafer, Kambiz Vafai, Marilyn Lightstone, Buoyancy-driven heat transfer enhancement in a two-dimensional enclosure utilizing nanofluids, International Journal of Heat and Mass Transfer 46 (2003) 3639–3653.

[12] A.H. Mahmoudi, M. Shahi, A.H. Raouf, A. Ghasemian, Numerical study of natural convection cooling of horizontal heat source mounted in a square cavity filled with nanofluid, International Communications in Heat and Mass Transfer 37 (2010) 1135–1141.

[13] E. Abu-Nada, Z. Masoud, H.F. Oztop, A. Campo, Effect of nanofluid variable properties on natural convection in enclosures, International Journal of Thermal Sciences 49 (2010) 479–491.

[14] F. Talebi, A.H. Mahmoudi, M. Shahi, Numerical study of mixed convection flows in a square lid-driven cavity utilizing nanofluid, International Communications in Heat and Mass Transfer 37 (2010) 79–90.

[15] M. Mahmoodi, Numerical simulation of free convection of a nanofluid in L-shaped cavities, International Journal of Thermal Sciences 50 (2011) 1731–1740.

[16] M. Shahi, A.H. Mahmoudi, F. Talebi, A numerical investigation of conjugated-natural convection heat transfer enhancement of a nanofluid in an annular tube driven by inner heat generating solid cylinder, International Communications in Heat and Mass Transfer 38 (2011) 533–542.

[17] E. Abu-Nada, Rayleigh-Bénard convection in nanofluids: effect of temperature dependent properties, International Journal of Thermal Sciences 50 (2011) 1720–1730.

[18] M. Rahimi, A.A. Ranjbar, M.J. Hosseini, M. Abdollahzadeh, Natural convection of nanoparticle–water mixture near its density inversion in a rectangular enclosure, International Communications in Heat and Mass Transfer, 10.1016/j.icheatmasstransfer.2011.09.010.

[19] B. Ghasemi, S.M. Aminossadati, Brownian motion of nanoparticles in a triangular enclosure with natural convection, International Journal of Thermal Sciences 49 (2010) 931–940.

[20] S.M. Aminossadati, B. Ghasemi, Enhanced natural convection in an isosceles triangular enclosure filled with a nanofluid, Computers and Mathematics with Applications 61 (2011) 1739–1753.

[21] Q. Sun, I. Pop, Free convection in a triangle cavity filled with a porous medium saturated with nanofluids with flush mounted heater on the wall, International Journal of Thermal Sciences 50 (2011) 2141–2153.

[22] M.A.A. Hamad, Analytical solution of natural convection flow of a nanofluid over a linearly stretching sheet in the presence of magnetic field, International Communications in Heat and Mass Transfer 38 (2011) 487–492.

[23] H. Aminfar, M. Mohammadpourfard, Y.N. Kahnamouei, A 3D numerical simulation of mixed convection of a magnetic nanofluid in the presence of non-uniform magnetic field in a vertical tube using two phase mixture model, Journal of Magnetism and Magnetic Materials 323 (2011) 1963–1972.

[24] B. Ghasemi, S.M. Aminossadati, A. Raisi, Magnetic field effect on natural convection in a nanofluid-filled square enclosure, International Journal of Thermal Sciences 50 (2011) 1748–1756.

[25] H.E. Patel, T. Pradeep, T. Sundararajan, A. Dasgupta, N. Dasgupta, S.K. Das, A microconvection model for thermal conductivity of nanofluid, Pramana-Journal of Physics 65 (2005) 863–869.

[26] H.C. Brinkman, The viscosity of concentrated suspensions and solutions, Journal of Chemical Physics 20 (1952) 571–581.

[27] J.C. Maxwell, A Treatise on Electricity and Magnetism, second ed. Oxford University Press, Cambridge, 1904, 435–441.

[28] J.H. Ferziger, M. Peric, Computational Method for Fluid Dynamics, Springer-Verlag (1999) New York.

[29] S.V. Patnkar, Numerical Heat Transfer and Fluid Flow, Hemisphere, New York (1980).

[30] G. De Vahl Davis, Natural convection of air in a square cavity a bench mark numerical solution, International Journal for Numerical Methods in Fluids 3 (1983) 249–264.

[31] M. Venkatachalappa, C.k. Subbaraya, Effect of a magnetic field on free convection in a rectangular enclosure, International Journal of Engineering Science 33 (1995) 1075–1084.

[32] V.A. Akinsete, T.A. Coleman, Heat transfer by steady laminar free convection in triangular enclosures, Internation Journal of Heat and Mass Transfer 25 (1982) 991–998.